Chemokines and the Arrest of Lymphocytes Rolling Under Flow Conditions

James J. Campbell, Joseph Hedrick, Albert Zlotnik, Michael A. Siani, Darren A. Thompson, Eugene C. Butcher

Circulating lymphocytes are recruited from the blood to the tissue by rolling along the endothelium until being stopped by a signaling event linked to the $G_i\alpha$ subunit of a heterotrimeric GTP-binding protein; that event then triggers rapid integrin-dependent adhesion. Four chemokines are now shown to induce such adhesion to intercellular adhesion molecule–1 and to induce arrest of rolling cells within 1 second under flow conditions similar to those of blood. SDF-1 (also called PBSF), 6-C-kine (also called Exodus-2), and MIP-3β (also called ELC or Exodus-3) induced adhesion of most circulating lymphocytes, including most $CD4^+$ T cells; and MIP-3α (also called LARC or Exodus-1) triggered adhesion of memory, but not naïve, $CD4^+$ T cells. Thus, chemokines can regulate the arrest of lymphocyte subsets under flowing conditions, which may allow them to control lymphocyte–endothelial cell recognition and lymphocyte recruitment in vivo.

The interaction between leukocytes in the circulation and endothelial cells lining the blood vessels is an important control point in the in vivo trafficking of specific leukocyte subsets. This interaction is mediated by a multistep process that, in many instances, involves (i) leukocyte rolling, (ii) rapid activation of leukocyte integrins, (iii) adhesion to endothelial ligands through activated integrins, and (iv) diapedesis (*1–7*). Steps (ii) and (iv) are often mediated through receptors linked to the pertussis toxin (PTX)–sensitive α subunit of G_i ($G_i\alpha$). Molecules that mediate step (ii) in neutrophils, monocytes, and eosinophils have been identified by both in vivo and in vitro methods, and they include interleukin-8 (IL-8), platelet-activating factor, leukotriene B_4, eotaxin, complement component 5a, and formyl peptide. Rapid adhesion of neutrophils occurs within seconds in vivo (*8, 9*). The rapidity of this event is important because leukocytes dynamically rolling through a site of inflammation (or a high endothelial venule of a secondary immune organ) must be stopped before exiting the area relevant to the adhesion-triggering stimulus.

Lymphocyte homing through high endothelial venules also involves a multistep decision cascade, including a PTX-sensitive rapid adhesion event (*10, 11*). Several chemokines—including macrophage inflammatory protein–1α (MIP-1α) (*12, 13*), MIP-1β (*12–14*), interferon-α inducible protein 10 (IP-10) (*12, 15*), and RANTES (regulated on activation, normal T expressed and secreted) (*12, 13, 15*)—have been shown to induce adhesion of human lymphocytes to endothelial cells or endothelial cell adhesion ligands. However, these responses were measured a minimum of 15 min (*12, 14*) to 1 hour (*13, 15*) after stimulation, and they often require a prior additional cellular stimulation, such as overnight treatment with cross-linked antibodies to CD3 (*13, 15*). Thus, chemokine-stimulated adhesion of this type may be more relevant to the behavior of immunoblasts within tissues than to the arrest of circulating lymphocytes. Indeed, we and others have shown that these chemokines are not effective in triggering rapid adhesion of normal lymphocytes similar to that observed during physiological lymphocyte–endothelial cell interactions in vivo (*16, 17*). However, lymphoid cells overexpressing transfected receptors for classical chemoattractants or for various chemokines respond efficiently in adhesion assays, which suggests that there is not a fundamental defect in the rapid integrin responsiveness of lymphocytes to chemoattractant stimulation (*18–20*).

We have now tested a battery of other chemokines with attractant activity for lymphocytes—including stromal cell–derived factor–1α (SDF-1α), SDF-1β (*21, 22*), C-X3-C-kine (also called fractalkine or neurotactin) (*23, 24*), MIP-3β (*25, 26*), 6-C-kine (*27*), MIP-3α (*25, 28–30*), DC-CK-1 (also called PARC) (*31, 32*), and TARC (*33*)—and compared them with chemokines more selective for myeloid cells or eosinophils. In initial experiments, a simple static assay (*18, 19*) was used to test the ability of these chemokines to trigger adhesion to integrin ligands at relatively early time points. Freshly isolated human peripheral lymphocytes were allowed to settle on mouse intercellular adhesion molecule–1 (ICAM-1)–coated glass (human LFA-1 cross-reacts with mouse ICAM-1), and were incubated with chemokine (1 μM) for various times. Unbound cells were then washed away, and bound cells were fixed and counted. SDF-1α, SDF-1β, MIP-3β, and 6-C-kine triggered rapid adhesion of

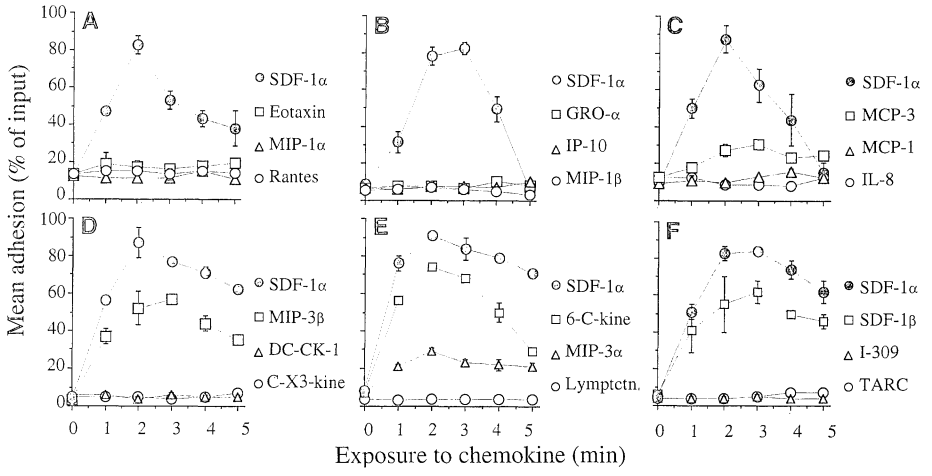

Fig. 1. Chemokine-triggered rapid adhesion of lymphocytes to ICAM-1. (**A** through **F**) The results of individual experiments assessing the ability of the indicated chemokines to trigger adhesion of human peripheral lymphocytes. SDF-1α was included in each assay for comparison (●). SDF-1α induced robust adhesion, but eotaxin, MIP-1α, MIP-1β, RANTES, MCP-1, GRO-α, IL-8, and IP-10 yielded no detectable binding at these early time points (upper panels). MCP-3 induced a low but reproducible response. Among other, more recently described chemokines (lower panels), 6-C-kine, MIP-3β, and SDF-1β gave robust responses; MIP-3α yielded reproducible binding of a smaller number of PBLs; and C-X3-C-kine, DC-CK-1, lymphotactin, I-309, and TARC were without effect.

J. J. Campbell and E. C. Butcher, Laboratory of Immunology and Vascular Biology, Department of Pathology, and Digestive Disease Center, Department of Medicine, Stanford University Medical School, Stanford, CA 94305, USA, and Center for Molecular Biology and Medicine, Veterans Affairs Palo Alto Health Care System, Palo Alto, CA 94304, USA.
J. Hedrick and A. Zlotnik, Department of Immunology, DNAX Research Institute of Molecular and Cellular Biology, Palo Alto, CA 94304, USA.
M. A. Siani and D. A. Thompson, Gryphon Sciences, South San Francisco, CA 94080, USA.

most peripheral lymphocytes (Fig. 1) (*34*). Monocyte chemoattractant protein–3 (MCP-3) and MIP-3α induced adhesion of a smaller percentage of cells, suggesting that they are less potent or activate a smaller subset of cells, or both. None of the other 12 chemokines tested triggered any detectable adhesion in these time frames. In all instances, adhesion was transient, returning to baseline within 5 to 8 min of exposure to chemokine (depending on the cell donor).

To examine whether the adhesion response was mediated by chemokine signaling through $G_i\alpha$-linked receptors, we assessed the effects of PTX, an enzyme that catalyzes the ADP-ribosylation of $G_i\alpha$ and inhibits downstream signaling. PTX treatment completely inhibited chemokine-induced adhesion to ICAM-1. PTX- and mock-treated cells responded similarly to phorbol ester, which activates lymphocyte integrins independently of G protein–linked receptors (Fig. 2A).

We next assessed the responsiveness of isolated $CD4^+$ T cells, positively selected to 99% purity by isolation with magnetic beads (*35*). Most $CD4^+$ T cells adhered to ICAM-1 in response to SDF-1α, 6-C-kine, and MIP-3β (Fig. 2B). There was no detectable response to MCP-3, whereas MIP-3α induced a small, but reproducible, response.

It was possible that the suboptimal MIP-3α response reflected selective activity in a specialized subset of lymphocytes. Unlike 6-C-kine and MIP-3β mRNAs, which are most abundant in organized lymphoid tissue such as lymph nodes (*25–27*), MIP-3α mRNA is most abundant in peripheral tissues such as lung and liver (*25*, *30*) and can be up-regulated by inflammatory mediators (*28*), suggesting selectivity for extralymphoid and inflammatory sites. Because trafficking to sites of inflammation is a characteristic of memory $CD4^+$ T cells (whereas naïve cells traffic predominantly through organized lymphoid tissues) (*7*, *36*), we next fractionated $CD4^+$ cells into memory and naïve phenotypes on the basis of their differential expression of CD45R isoforms (Fig. 2C) (*37*). Only $CD4^+$ cells of the memory phenotype responded detectably to MIP-3α, whereas both subsets responded to SDF-1α. Thus, subsets responded differentially to the proadhesive activity of chemokines. In this context, it should be emphasized that minor subsets of circulating cells (such as immunoblasts) may display patterns of chemokine-triggered arrest distinct from those of the major population of resting lymphocytes studied here.

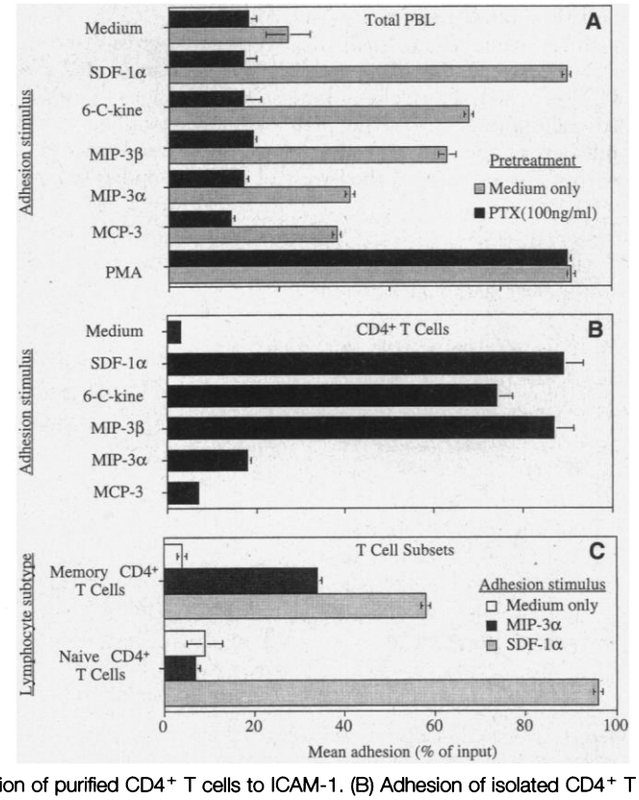

Fig. 2. (**A**) Inhibition by PTX of chemokine-triggered adhesion of human lymphocytes to ICAM-1. Cells were incubated in control medium (gray bars) or with PTX (100 ng/ml) (black bars) for 2 hours, after which adhesion assays were performed as in Fig. 1. Cells were stimulated with control medium, with the indicated chemokine (1 μM), or with phorbol 12-myristate 13-acetate (PMA) (100 ng/ml). Chemokine-induced binding was assayed after 2 min and PMA-induced binding after 25 min, the times of maximal response in each instance. In all instances, the cells were in contact with the ICAM-1–coated surface for equal amounts of time. This experiment is representative of results obtained with cells from two independent donors. Error bars indicate range of duplicate wells. PTX was obtained from List Laboratories (Campbell, California). (**B** and **C**). Chemokine-induced rapid adhesion of purified $CD4^+$ T cells to ICAM-1. (B) Adhesion of isolated $CD4^+$ T cells to ICAM-1 in response to various chemokines. The adhesion assay was performed as in (A). (C) $CD4^+$ T cells were further fractionated into $CD45RA^+CD45RO^-$ and $CD45RA^-CD45RO^+$ subsets by depletion with antibodies to CD45RO or to CD45RA, respectively, and chemokine-induced binding was assayed 2 min after addition of agonist. Experiments presented are representative of results obtained with cells from three independent donors. Error bars indicate range of duplicate wells.

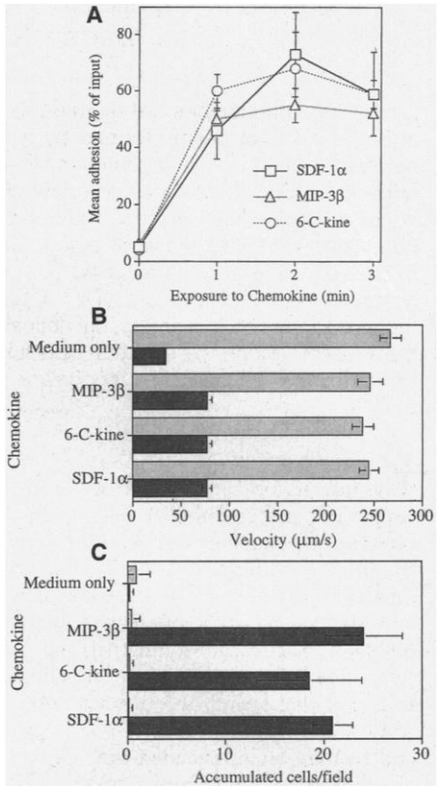

Fig. 3. Chemokine-induced adhesion of murine lymphocytes under shear. (**A**) Response of mouse lymph node cells to SDF-1α, 6-C-kine, and MIP-3β in the static ICAM-1 adhesion assay. A mixture of lymphocytes from axillary, cervical, inguinal, and mesenteric lymph nodes from Balb/c mice (4 to 6 weeks old) was tested as in Fig. 1. Error bars indicate range of duplicate wells. (**B**) Comparison of rolling speeds at a shear of 2 dynes/cm^2 of murine lymphocytes in capillaries coated with PNAd alone or PNAd plus chemokine. For each experiment, the mean velocity of 10 tumbling cells (cells traveling in the focal plane of an uncoated region of the capillary) was calculated (gray bars). Rolling speed was calculated for 25 individual cells between 2 and 4 min after the start of the assay (black bars). Interaction of cells with PNAd plus chemokine was less efficient than that with PNAd alone; given that chemokines did not induce a loss of L-selectin expression on lymphocytes, possible explanations for this observation include blockade of L-selectin–binding components within PNAd by the heparin-binding domain of the chemokine or disruption of the microvillous structures that bear L-selectin on the lymphocytes themselves. Error bars indicate SEM. (**C**) The number of cells that adhered (remained arrested for ≥1 min) on PNAd plus chemokine (gray bars) compared with the number that adhered on ICAM-1 plus PNAd plus chemokine (black bars). Eight different fields were counted between 4 and 6 min after the start of the assay. Error bars indicate the SD of these counts. Data are representative of three separate experiments.

Lymphocyte adhesion and arrest on endothelium in vivo occur in the context of blood flow. To assess the ability of chemokines to trigger arrest under physiological shear and to estimate more precisely the time required for induction of firm arrest, we turned to an in vitro flow system (Fig. 3) (*38–41*). Capillary tubes were coated with immuno-isolated peripheral node addressin (PNAd) or ICAM-1, or both, with or without chemokines. Mouse lymph node lymphocytes were then passed through the tubes at a shear of 2 dynes/cm^2. PNAd is a ligand for the microvillus tethering receptor L-selectin and supports efficient contact initiation and rolling, but not firm arrest, of L-selectin$^+$ cells (which include most lymphocytes, with the exception of a subset of memory T and B cells) (*7*). ICAM-1 is a ligand for the lymphocyte integrin LFA-1, whose engagement is dependent both on prior tethering through microvillus receptors and on integrin-activating signals (*7*, *39*). As shown previously (*39*), lymphocytes rolled but did not stop on PNAd or on PNAd plus ICAM-1 (Fig. 3, B and C). Lymphocytes only stopped when exposed to capillaries coated with PNAd, ICAM-1, and either SDF-1α, MIP-3β, or 6-C-kine. The absence of adhesion to PNAd plus chemokine without ICAM-1 indicates that adhesion was dependent on the latter, and that the cells were not binding to any of the diverse proteins that constitute PNAd. It also rules out a simple mechanical adhesion between the chemokine-coated surface and the chemokine receptors on the cells.

The rolling of representative lymphocytes on PNAd alone or with chemokine (Fig. 4, A through D), and the deceleration of cells on the surfaces coated with PNAd, ICAM-1, and chemokine (Fig. 4, E through G), were plotted. For the experiments shown, the deceleration time of 10 randomly chosen cells that entered the field at tumbling velocity and arrested for >1 min was calculated. The mean deceleration times were 380, 510, and 430 ms for cells arresting on MIP-3β, 6-C-kine, and SDF-1α, respectively. For each chemokine, several cells arrested from 100 μm/s in less time than that between video frames (≤30 ms). The maximum rolling time before arrest was 1.6, 1.4, and 1.0 s for MIP-3β, 6-C-kine, and SDF-1α, respectively. MIP-3α did not induce arrest of significant numbers of lymphocytes in the presence of PNAd and ICAM-1; however, this lack of effect may reflect a paucity of MIP-3α–responsive cells in the L-selectin$^+$ memory subset, because in separate preliminary studies MIP-3α did trigger arrest of a subset of cells rolling on a surface coated with MAdCAM-1 [which can support tethering and rolling through the integrin $\alpha^4\beta^7$ (*41*)] plus ICAM-1.

The receptor systems that mediate the multistep process of leukocyte–endothelial cell interaction have evolved to meet the deceleration requirements of cells traveling at high speed through the vertebrate circulatory system. For example, adhesion molecules that mediate the tethering and rolling steps are concentrated on the tips of microvilli, the sites of initial lymphocyte contact with the vascular endothelium (*7*). The participation of lymphocyte chemoattractant receptors, especially receptors for chemokines, in the rapid physiological conversion of rolling behavior to firm integrin-dependent arrest has been suggested but unconfirmed since the original proposal of a general multistep model of leukocyte–endothelial cell interaction. The identification of chemokines that can trigger almost immediate integrin-dependent arrest of lymphocytes under physiological shear not only provides an important confirmation of the general role of chemokines as adhesion triggers in leukocyte–endothelial cell interactions but broadens the potential for control of lymphocyte trafficking by this diverse emerging family of chemoattractants.

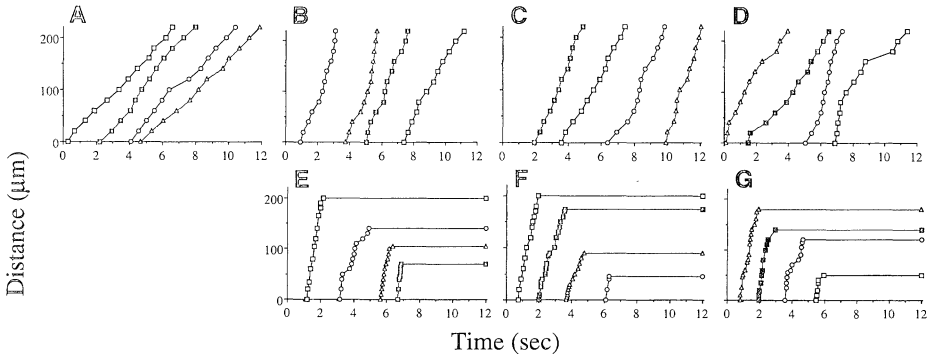

Fig. 4. Lymphocyte behavior in the flow assay. In these plots, the slope of the line is proportional to the velocity of the cell. The behavior of four representative cells is shown for each assay. The *y* axis indicates the length of the microscopic field (220 μm), with zero as the downstream entry into the field and 220 as the upstream exit from the field. The time at which the cell enters the field is arbitrary. Capillary tubes were coated with a combination of PNAd plus either medium alone (**A**), MIP-3β (**B**), 6-C-kine (**C**), or SDF-1α (**D**), or with ICAM-1 plus PNAd plus either MIP-3β (**E**), 6-C-kine (**F**), or SDF-1α (**G**). Cells were passed through the tube at a shear force of 2.0 dynes/cm^2. The mean velocities of tumbling and rolling cells from experiments (A) through (D) are shown in Fig. 3B. The mean (± SD) deceleration times [time necessary to decelerate from a speed 1 SD greater than the mean rolling speed (~100 μm/s) to a complete stop] for 10 cells in each experiment were as follows: MIP-3β (E), 380 ± 490 ms (minimum, ≤30 ms; maximum, 1.6 s); 6-C-kine (F), 510 ± 470 ms (minimum, ≤30 ms; maximum, 1.4 s); SDF-1α (G), 430 ± 340 ms (minimum, ≤30 ms; maximum, 970 ms).

REFERENCES AND NOTES

1. E. C. Butcher, *Cell* **67**, 1033 (1991).
2. Y. Shimuzu, W. Newman, Y. Tanaka, S. Shaw, *Immunol. Today* **13**, 106 (1992).
3. T. M. Carlos and J. M. Harlan, *Blood* **84**, 2068 (1994).
4. T. J. Schall and K. B. Bacon, *Curr. Opin. Immunol.* **6**, 865 (1994).
5. A. Imhof and D. Dunon, *Adv. Immunol.* **58**, 345 (1995).
6. T. A. Springer, *Annu. Rev. Physiol.* **57**, 827 (1995).
7. E. C. Butcher and L. J. Picker, *Science* **272**, 60 (1996).
8. U. von Andrian *et al.*, *Am. J. Physiol.* **263**, H1034 (1992).
9. U. R. von Andrian *et al.*, *Proc. Natl. Acad. Sci. U.S.A.* **88**, 7538 (1991).
10. R. F. Bargatze and E. C. Butcher, *J. Exp. Med.* **178**, 367 (1993).
11. R. A. Warnock, S. Askari, E. C. Butcher, U. H. von Andrian, *ibid.*, in press.
12. A. R. Lloyd, J. J. Oppenheim, D. J. Kelvin, D. D. Taub, *J. Immunol.* **156**, 932 (1996).
13. D. D. Taub, K. Conlon, A. R. Lloyd, J. J. Oppenheim, D. J. Kelvin, *Science* **260**, 355 (1993).
14. Y. Tanaka *et al.*, *Nature* **361**, 79 (1993).
15. D. D. Taub *et al.*, *J. Exp. Med.* **177**, 1809 (1993).
16. M. W. Carr, R. Alon, T. A. Springer, *Immunity* **4**, 179 (1996).
17. R. F. Bargatze, thesis, Montana State University, Bozeman, MT (1994).
18. S. Honda *et al.*, *J. Immunol.* **152**, 4026 (1994).
19. J. J. Campbell, S. Qin, K. B. Bacon, C. R. Mackay, E. C. Butcher, *J. Cell Biol.* **134**, 255 (1996).
20. J. J. Campbell, E. F. Foxman, E. C. Butcher, *Eur. J. Immunol.* **27**, 2471 (1997).
21. K. Tashiro *et al.*, *Science* **261**, 600 (1993).
22. C. C. Bleul, R. C. Fuhlbrigge, J. M. Casanovas, A. Aiuti, T. A. Springer, *J. Exp. Med.* **184**, 1101 (1996).
23. J. F. Bazan *et al.*, *Nature* **385**, 640 (1997).
24. Y. Pan *et al.*, *ibid.* **387**, 611 (1997).
25. D. L. Rossi, A. P. Vicari, K. Franz-Bacon, T. McClanahan, A. Zlotnik, *J. Immunol.* **158**, 1033 (1997).
26. R. Yoshida *et al.*, *J. Biol. Chem.* **272**, 13803 (1997).
27. J. A. Hedrick and A. Zlotnik, *J. Immunol.* **159**, 1589 (1997).
28. R. Hromas *et al.*, *Blood* **89**, 3315 (1997).
29. M. Baba *et al.*, *J. Biol. Chem.* **272**, 14893 (1997).
30. K. Heishima *et al.*, *ibid.*, p. 5846.
31. G. J. Adema *et al.*, *Nature* **387**, 713 (1997).
32. K. Heishima *et al.*, *J. Immunol.* **159**, 1140 (1997).
33. T. Imai, M. Baba, M. Nishimura, S. Takagi, O. Yoshie, *J. Biol. Chem.* **272**, 15036 (1997).
34. Human lymphocytes were allowed to settle on the ICAM-1–coated surface of a multiwell glass slide. ICAM-1 was coated to a density of ~1000 sites per square micrometer. After cell settling, the indicated chemokines were added to a final concentration of 1 μM. The slides were washed at the indicated times to remove nonadherent cells, and bound cells were then fixed in 1.5% glutaraldehyde. The adherent cells in the microscopic field proximal to the site of chemoattractant addition were counted. Error bars in Fig. 1 indicate the range of duplicate wells. Each experiment is

representative of results from at least two independent donors. ICAM-1 was obtained from mouse spleens by the tissue lysis procedure as previously described (*18*) and was affinity-purified on a monoclonal antibody BE-29G1–Sepharose (Pharmacia) column. Human peripheral blood mononuclear cells were isolated from healthy donors as described [C. P. Nielson, R. E. Vestal, R. J. Sturm, R. Haeslip, *J. Allergy Clin. Immunol.* **88**, 801 (1990)]. Monocytes were removed from the cells by adherence to a T-175 culture flask (Nunc, Demark) at 37°C and 8% CO_2 for 30 min in RPMI 1640 medium supplemented with 10% calf serum. Recombinant human eotaxin, MIP-1α, MIP-1β, RANTES, MCP-1, MCP-3, IP-10, IL-8, GRO-α, C-X3-C-kine, DC-CK-1, MIP-3α, MIP-3β, 6-C-kine, I-309, SDF-1β, lymphotactin, and TARC were obtained from R&D Systems (Minneapolis, MN) or PeproTech (Rocky Hill, NJ). Recombinant IL-8 was also provided by A. Rott (Sandoz, Vienna). Synthetic human SDF-1α, MIP-3α, MIP-3β, TARC, and C-X3-C-kine were also prepared by two of the authors (M.A.S. and D.A.T.) by chemical ligation [P. E. Dawson, T. W. Muir, I. Clark-Lewis, S. H. B. Kent, *Science* **266**, 776 (1994). Synthetic SDF-1α was also provided by I. Clark-Lewis. Chemokines were shown to be active by chemotaxis of human peripheral blood lymphocytes, eosinophils, or neutrophils, or of chemokine receptor–overexpressing lymphoma cell lines. There were no detectable differences among chemokines obtained from different sources in these assays.

35. $CD4^+$ cells were purified with the use of anti-CD4 Dynabeads and the DETACH-a-BEAD system (Dynal, Lake Success, NY). Mouse monoclonal antibodies to human CD45RO (clone UCHL1) and to human CD45RA (clone HI100) were obtained from PharMingen (San Diego, CA). Cells coated with these monoclonal antibodies were removed by incubation with microbeads conjugated with antibodies to mouse immunoglobulin, followed by magnetic depletion (Miltenyi Biotec, Auburn, CA). A portion of each processed cell subpopulation was stained with directly conjugated monoclonal antibodies and analyzed by flow cytometry to ascertain purity, which was ~99% for $CD4^+$ cells and ~97% for both $CD45RA^-$ $CD45RO^+$ and $CD45RA^+$ $CD45RO^-$ subpopulations.
36. C. R. Mackay, *Adv. Immunol.* **53**, 217 (1993).
37. M. E. Sanders *et al.*, *J. Immunol.* **140**, 1401 (1988).
38. E. L. Berg, L. M. McEvoy, C. Berlin, E. C. Butcher, *Nature* **366**, 695 (1993); U. H. von Andrian, S. R. Hasslen, R. D. Nelson, S. L. Erlandsen, E. C. Butcher, *Cell* **82**, 989 (1995).
39. M. B. Lawrence, E. L. Berg, E. C. Butcher, T. A. Springer, *Eur. J. Immunol.* **25**, 1025 (1995).
40. PNAd was obtained from human tonsils with the tissue lysis procedure previously described (*18*) and was affinity-purified on a monoclonal antibody MECA-79–Sepharose column. The inside walls of 100-μl microcap capillary tubes (Drummond, Broomall, PA) were coated with PNAd or a combination of PNAd plus ICAM-1. For double coatings, the tubes were coated first with 10 μl of diluted ICAM-1 for 8 hours at 4°C, the unbound ICAM-1 was removed, and the tubes were then coated with diluted PNAd by incubation overnight at 4°C. For single PNAd coating, only the second half of this procedure was performed. Before flow experiments, unbound PNAd was removed and the entire inside of the capillary was exposed to 100% calf serum at room temperature for 5 min. To cocoat the PNAd–ICAM-1 areas with immobilized chemokine (or medium alone as a control), we added 10 μl of 2 μM chemokine (in equilibrated RPMI 1640 with 10% calf serum) through the downstream end of the capillary and coaxed it into the same position as the area coated with PNAd and ICAM-1. Care was taken that no chemokine touched the capillary upstream of the PNAd and ICAM-1. The tube was then incubated for 5 min at ambient temperature. Immediately before the experiment, the unbound chemokine was washed out through the downstream end of the tube by infusing 5 ml of complete medium into the upstream end. Washing in this direction prevented chemokine from contacting the upstream areas. Cells were passed through the capillary in complete medium at a density of 1.5×10^6 per milliliter. The rate of flow was controlled by a Harvard 33 syringe pump (Harvard Apparatus, South Natick, MA). Experiments were performed at a flow rate of 1250 μl/min, which creates a wall shear stress of ~2.0 dynes/cm^2 for a capillary with an inner diameter of 1.025 mm, as calculated from Poiseuille's law for newtonian fluids with a viscosity of 0.01 poise. {Wall shear stress (dyne cm^2) = mean flow velocity (mm/s) × [8/tube diameter (mm)] × viscosity (poise).} The interactions of cells with the coated areas were recorded on videotape, and the behavior of individual cells was analyzed frame by frame.
41. C. Berlin *et al.*, *Cell* **80**, 413 (1995).
42. We thank I. Clark-Lewis, U. H. von Andrian, and D. P. Andrew for synthetic SDF-1α, PNAd, and ICAM-1, respectively, used in preliminary experiments; E. P. Bowman, K. Youngman, and M. Hubbe for help with preliminary experiments and discussions; L. Rott and G. Haraldson for advice on cell separation; and S. Haugejorden-Brown, E. P. Bowman, E. F. Foxman, and R. A. Warnock for critical reading of the manuscript. Supported by NIH grant GM37734 and an award from the Department of Veterans Affairs (E.C.B.); NIH grant DK38707 to the FACS Core Facility of the Stanford Digestive Disease Center, and NIH Cancer Etiology, Prevention, Detection, and Diagnosis grant 5T32CA090302, NIH grant 1F32AI08930, and the Arthritis Foundation (J.J.C.).

6 October 1997; accepted 2 December 1997

Structure of the HIV-1 Nucleocapsid Protein Bound to the SL3 Ψ-RNA Recognition Element

Roberto N. De Guzman, Zheng Rong Wu, Chelsea C. Stalling, Lucia Pappalardo, Philip N. Borer,* Michael F. Summers*

The three-dimensional structure of the human immunodeficiency virus–type 1 (HIV-1) nucleocapsid protein (NC) bound to the SL3 stem-loop recognition element of the genomic Ψ RNA packaging signal has been determined by heteronuclear magnetic resonance spectroscopy. Tight binding (dissociation constant, ~100 nM) is mediated by specific interactions between the amino- and carboxyl-terminal CCHC-type zinc knuckles of the NC protein and the G^7 and G^9 nucleotide bases, respectively, of the G^6-G^7-A^8-G^9 RNA tetraloop. A^8 packs against the amino-terminal knuckle and forms a hydrogen bond with conserved Arg^{32}, and residues Lys^3 to Arg^{10} of NC form a 3_{10} helix that binds to the major groove of the RNA stem and also packs against the amino-terminal zinc knuckle. The structure provides insights into the mechanism of viral genome recognition, explains extensive amino acid conservation within NC, and serves as a basis for the development of inhibitors designed to interfere with genome encapsidation.

All retroviruses encode a gag polyprotein that is produced in the host cell during the late stages of the infectious cycle and directs the encapsidation of two copies of the unspliced viral genome during virus assembly and budding (*1*). Concomitant with budding, the gag polyproteins are cleaved by the viral protease into the matrix (MA), capsid (CA), and nucleocapsid (NC) proteins, which rearrange during maturation to form infectious particles (*2*). Except for the spumaviruses, all retroviral NC proteins contain one or two CCHC-type zinc knuckle domains (Cys-X_2-Cys-X_4-His-X_4-Cys, where X = variable amino acid) (*3*) (Fig. 1A). These domains are critical for viral replication and participate directly in genome recognition and encapsidation (*4*, *5*). Mutations that abolish zinc binding lead to noninfectious virions that lack their genomes (*4*, *6*), and mutations of conservatively substituted hydrophobic residues within the CCHC arrays can alter RNA packaging specificity (*5*). In addition, entire NC domains of HIV-1 and Moloney murine leukemia virus (MoMuLV) have been swapped, resulting in the specific packaging of the non-native genomes (*6*).

Recognition of the HIV-1 genome occurs by means of interactions between NC and a ~120-nucleotide region of the unspliced viral RNA known as the Ψ-site, which is located between the 5′ long terminal repeat and the *gag* initiation codon (*7*). Extensive site-directed mutagenesis, chemical modification, nuclease accessibility mapping, and free energy computational studies indicate that the HIV-1 Ψ-site contains four stem-loop structures, denoted SL1 through SL4 (Fig. 1B) (*8*–*13*). Although mutagenesis experiments indicate that all four of these structures are important for efficient encapsidation (*13*, *14*), SL3 is of particular interest because its sequence is highly conserved among different strains of HIV-1 (*10*) despite heterogeneity at adjacent positions, and because linkage of SL3 to heterologous RNAs is sufficient to direct their recogni-

R. N. De Guzman, Z. R. Wu, C. C. Stalling, M. F. Summers, Howard Hughes Medical Institute and Department of Chemistry and Biochemistry, University of Maryland–Baltimore County (UMBC), 1000 Hilltop Circle, Baltimore, MD 21250, USA.
L. Pappalardo and P. N. Borer, Department of Chemistry, Syracuse University, Syracuse, NY 13244, USA.
*To whom correspondence should be addressed.